Cell Reports

Report

IL4/STAT6 Signaling Activates Neural Stem Cell Proliferation and Neurogenesis upon Amyloid-β42 Aggregation in Adult Zebrafish Brain

Graphical Abstract

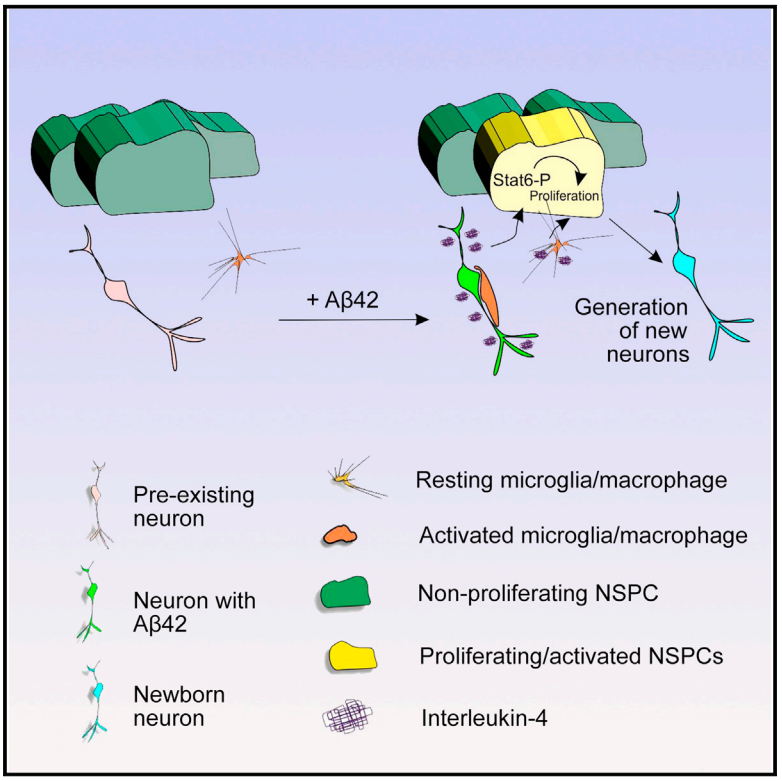

Authors

Prabesh Bhattarai, Alvin Kuriakose Thomas, Mehmet Ilyas Cosacak, ..., Andreas Dahl, Yixin Zhang, Caghan Kizil

Correspondence

caghan.kizil@dzne.de

In Brief

Bhattarai et al. shows that adult zebrafish brain displays Alzheimer's disease-like phenotypes after Amyloid-β42 (Aβ42) aggregation. Aβ42 can also activate neural stem cell proliferation and neurogenesis. Interleukin-4, which induces STAT6 phosphorylation, is a key factor for mediating the neuro-immune crosstalk between diseased neurons, immune cells, and stem cells.

Highlights

- Amyloid-β42 (Aβ42) forms aggregates in neurons of adult zebrafish brain
- Aβ42 causes apoptosis, inflammation, synaptic loss, and memory deficits in zebrafish
- Aβ42 leads to interleukin-4 (IL4) upregulation in neurons and microglia
- IL4/STAT6 signaling induces neural stem cell proliferation

Accession Numbers

GSE74326

Bhattarai et al., 2016, Cell Reports *17*, 941–948
October 18, 2016
http://dx.doi.org/10.1016/j.celrep.2016.09.075

CellPress

Cell Reports
Report

IL4/STAT6 Signaling Activates Neural Stem Cell Proliferation and Neurogenesis upon Amyloid-β42 Aggregation in Adult Zebrafish Brain

Prabesh Bhattarai,[1,2] Alvin Kuriakose Thomas,[3] Mehmet Ilyas Cosacak,[1,2] Christos Papadimitriou,[1,2] Violeta Mashkaryan,[1,2] Cynthia Froc,[4] Susanne Reinhardt,[2,5] Thomas Kurth,[2,5] Andreas Dahl,[2,5] Yixin Zhang,[3] and Caghan Kizil[1,2,6,*]

[1]German Centre for Neurodegenerative Diseases (DZNE) Dresden, Helmholtz Association, Arnoldstrasse 18, 01307 Dresden, Germany
[2]DFG-Center for Regenerative Therapies Dresden (CRTD), Cluster of Excellence, TU Dresden, Fetscherstrasse 105, 01307 Dresden, Germany
[3]B CUBE, Center for Molecular Bioengineering, TU Dresden, Arnoldstrasse 18, 01307, Dresden, Germany
[4]Neuroscience Paris-Saclay Institute, AMATrace Platform, UMR 9197, CNRS, Avenue de la Terrasse, 91190 Gif-sur-Yvette, France
[5]Biotechnology Center (BIOTEC), TU Dresden, Tatzberg 47, 01307 Dresden, Germany
[6]Lead Contact
*Correspondence: caghan.kizil@dzne.de
http://dx.doi.org/10.1016/j.celrep.2016.09.075

SUMMARY

Human brains are prone to neurodegeneration, given that endogenous neural stem/progenitor cells (NSPCs) fail to support neurogenesis. To investigate the molecular programs potentially mediating neurodegeneration-induced NSPC plasticity in regenerating organisms, we generated an Amyloid-β42 (Aβ42)-dependent neurotoxic model in adult zebrafish brain through cerebroventricular microinjection of cell-penetrating Aβ42 derivatives. Aβ42 deposits in neurons and causes phenotypes reminiscent of amyloid pathophysiology: apoptosis, microglial activation, synaptic degeneration, and learning deficits. Aβ42 also induces NSPC proliferation and enhanced neurogenesis. Interleukin-4 (IL4) is activated primarily in neurons and microglia/macrophages in response to Aβ42 and is sufficient to increase NSPC proliferation and neurogenesis via STAT6 phosphorylation through the IL4 receptor in NSPCs. Our results reveal a crosstalk between neurons and immune cells mediated by IL4/STAT6 signaling, which induces NSPC plasticity in zebrafish brains.

INTRODUCTION

Human brains are prone to neurodegenerative disorders, which cannot be counteracted by the regeneration of lost cells. Patients with neurodegenerative conditions progressively lose neurons yet cannot form new ones; namely, they lack the proper differentiation/survival response of stem-cell-derived neurons (Demars et al., 2010). Therefore, inducing a functional "proliferation-differentiation-survival cascade" upon neurodegenerative conditions in mammalian neural stem cells, which otherwise bear neurogenic capacity (Doetsch et al., 1997), could serve as a therapeutic tool. In nature, several vertebrates such as zebrafish bear widespread regenerative ability (Tanaka and Ferretti, 2009), and studies aiming to understand the natural competency of regeneration in zebrafish would be clinically important.

Inflammatory conditions in neurodegenerative diseases are multi-faceted and have pleitropic effects on microglia, neurons, and neural stem/progenitor cells (NSPCs) (Das and Basu, 2008; Kizil et al., 2015b). Inflammation has beneficial and detrimental effects on stem cells, and this ambiguity could be due to the automodulatory effects of inflammatory milieu on microglia, which indirectly affect the stem cell behavior (Ekdahl et al., 2009; Kokaia et al., 2012; Kyritsis et al., 2014; Monje et al., 2003; Schwartz and Shechter, 2010). There is increasing evidence that neural stem cells also use immune-type signaling molecules, which might set up a direct interaction of neurons and microglia with the neural stem cells (Ben-Hur et al., 2003; Ekdahl et al., 2009; Kizil et al., 2012a, 2012c; Kyritsis et al., 2012). Therefore, in vivo assay systems to address the direct role of inflammation on stem cells are necessary. Zebrafish offers an excellent tool due to its regenerative ability in the CNS (Chapouton et al., 2007; Kizil et al., 2012b). Also, neurodegeneration models in adult zebrafish brain could help in investigating whether neural stem/progenitor cells (NSPCs) would be activated and whether we could find out the molecular differences between zebrafish and mammalian NSPCs to harness them for regenerative therapies (Cosacak et al., 2015). Thus, we generated a rapid and reproducible model of neurodegeneration in adult zebrafish brain using Amyloid-β42 (Aβ42), which is the hallmark of Alzheimer's disease pathology (Haass and Selkoe, 2007). We investigated the response of NSPCs after amyloid toxicity and the molecular programs that could govern this response.

RESULTS AND DISCUSSION

Aβ42 Accumulates in Neurons of Adult Zebrafish Brain

To introduce Aβ42 peptides into adult zebrafish brain, we used human Aβ42 uncoupled or coupled to two cell-penetrating

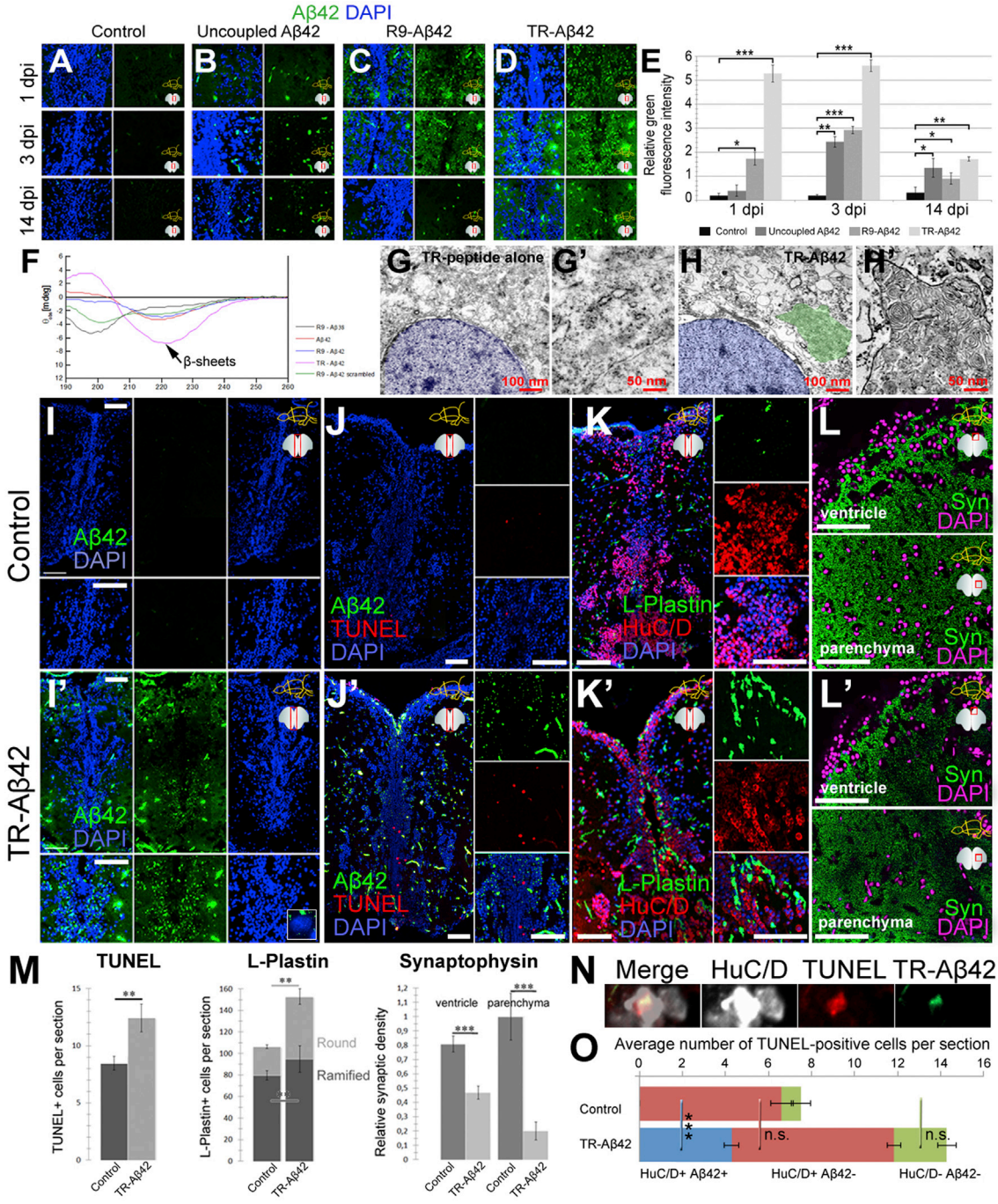

Figure 1. Aβ42 Injection Paradigm and Aggregation-Dependent Phenotypes in Adult Zebrafish Brain

(A) Immunohistochemistry (IHC) for Aβ42 in control brains at 1, 3, and 14 days post-injection (dpi) of PBS. Right panels: green channel.

(B–D) IHC for Aβ42 in brains injected with uncoupled Aβ42 (B), R9-Aβ42 (C), or TR-Aβ42 (D).

(E) Quantification for green fluorescence intensity as a measure of amyloid deposition.

(F) CD spectra for all Aβ42 versions in buffer (PBS). Aβ42 peptides show β sheet formation.

(G–H') Electron micrographs of TR-alone- (G) and TR-Aβ42-injected (H) brains. Blue, nucleus; green, amyloid. (G' and H') Higher magnification of perinuclear regions with Aβ42.

(I and I') IHC for Aβ42 in control (I) and TR-Aβ42-injected (I') brains. Green and DAPI are shown separately.

(J and J') TUNEL for control (J) and TR-Aβ42-injected (J') brains. Insets: single channels of a close-up region.

(K and K') HuC/D and L-Plastin in control (K) and TR-Aβ42-injected (K') brains.

(L and L') Synaptophysin in control (L) and TR-Aβ42-injected (L') brains.

(legend continued on next page)

peptides, poly-arginine (R9-Aβ42) and transportan (TR-Aβ42) (Kizil et al., 2015a). We detected Aβ42 in zebrafish brain at 1, 3, and 14 days post-injection (dpi) (Figures 1A–1D). All peptides accumulate with different temporal dynamics, TR-Aβ42 being the fastest (Figure 1E). To determine whether coupling Aβ42 to penetrating peptides affected their capacity to form β sheets, we performed circular dichroism (CD) and aggregation studies (Figures 1F and S1A–S1G). Although all Aβ42 versions form β sheets, TR-Aβ42 is more potent (Figure 1F). TR peptide alone is also not toxic to the cells (Figures S1H–S1M).

To test whether injected TR-Aβ42 would form β sheets, we performed electron microscopy in TR- (Figures 1G and 1G') or TR-Aβ42-injected brains (Figures 1H and 1H'). TR-Aβ42 forms intracellular β sheet aggregations and could be used for our subsequent analyses as a new model of amyloidosis.

Aβ42 Leads to Neurodegeneration Phenotypes in Adult Zebrafish Brain

In humans, Aβ42 deposition causes cell death (Shaked et al., 2006), unlike many animal models (Duff et al., 1996). To check whether TR-Aβ42 in adult zebrafish brain (Figures 1I and 1I') would cause cell death, we performed TUNEL staining (Figures 1J and 1J'). TR-Aβ42 significantly increased apoptosis (Figure 1M) more than uncoupled Aβ42 and R9-Aβ42 (Figure S1N).

A hallmark of Aβ42 in mammalian models is the activation of microglia/macrophages (μg/μØ) (Wyss-Coray, 2006). To test whether in zebrafish μg/μØ would be activated after Aβ42 (either through recruitment from periphery or mobilization of brain-resident cells), we measured the number and activation state (based on morphology) of μg/μØ after Aβ42 injection (Figures 1K and 1K'). Amyloid deposition significantly and persistently increased the number of amoeboid μg/μØ after all Aβ42 versions (Figure S1O), but was most pronounced after TR-Aβ42 (Figure 1M), suggesting that Aβ42 leads to immune response and pro-inflammatory gene expression (Figure S1T) in zebrafish brain.

Aβ42 causes synaptic degeneration and memory deficits in mammalian brains (Selkoe, 2002). To investigate whether TR-Aβ42 in adult zebrafish brain would affect synaptic connections, we detected synaptophysin after injection of TR-Aβ42. TR-Aβ42 reduces synaptophysin-positive synapses (Figures 1L–1M) and synaptic gene expression (Figure S1U), suggesting that synapses degenerate.

To investigate whether Aβ42 accumulates in neurons that undergo apoptosis, we detected HuC/D, TUNEL, and TR-Aβ42 (Figure 1N). Quantification of TUNEL-positive cells showed that the only significantly increasing cell population was Aβ42-containing neurons (HuC/D-Aβ42-TUNEL triple-positive cells) (Figure 1O), indicating that Aβ42-containing neurons specifically undergo apoptosis after Aβ42 injection.

To test the specificity of the toxicity of Aβ42, we injected Aβ38—a short Aβ peptide not found in patients' plaques and having higher solubility than Aβ42—or scrambled Aβ42 (Figure S1Q). Compared to controls, TR-Aβ38 and scrambled Aβ42 did not alter cell death, microglial activation, synaptophysin immunoreactivity, or the homeostatic proliferation of NSPCs (Figures S1R and S1S), suggesting that, in zebrafish brain, TR-Aβ42 is specifically causing toxicity, cell death, inflammation, and synaptic loss reminiscent of mammalian brains.

One symptom of Alzheimer's disease is memory deficits and cognitive decline (Chen et al., 2000). To examine whether Aβ42 in adult zebrafish brain would lead to learning deficits, we performed a passive avoidance test (Figures S2A–S2C). Although control and TR-Aβ42-injected fish swam normally before conditioning (Figure S2D), control fish significantly avoided the side paired with the electric shock after 3 days of conditioning, while TR-Aβ42-injected fish did not (Figure S2E). The swimming speed of TR-Aβ42-injected fish in the shock-paired compartment was slower than that of control fish (Figure S2E), suggesting a lower anxiety response. These results demonstrate that Aβ42-mediated neurodegeneration and synaptic loss impairs zebrafish learning.

Aβ42 Leads to NSPC Proliferation and Neurogenesis

Compared to control brains, TR-Aβ42 leads to significantly elevated levels of progenitor cell proliferation (Figures 2A–2C). Other Aβ42 versions, but not Aβ38, show this effect to a lesser extent (Figures S1P–S1S). To investigate whether the increase in progenitor proliferation leads to neurogenesis, we performed bromodeoxyuridine (BrdU) pulse-chase analyses labeling the proliferating cells at earlier phases after TR-Aβ42 injection and determining their progeny (Figures 2D–2G). Compared to controls, TR-Aβ42-injected zebrafish generated significantly increased numbers of neurons that migrated longer distances (Figures 2F and 2G). We also tested the effects of Aβ42 on neurogenesis by using a mature neuronal marker, HuC/D (Figures 2H–2J), and observed a significant increase in the number of newborn neurons (Figure 2J).

To address whether TR-Aβ42-injected fish would regain learning functions, we performed conditional learning tests at 12 weeks post-injection (wpi) with the same fish used for previous tests (Figure S2F). The control fish froze after the first electric shock and could not be experimented on further (data not shown). TR-Aβ42-injected fish failed to fully restore the behavioral phenotype. This suggests that restoration of learning capacity would either take longer time or more intense conditioning schemes.

TUNEL, L-plastin, synaptophysin, and S100/PCNA (proliferating cell nuclear antigen) stainings in a longitudinal manner from 1 to 30 dpi (Figure S3) showed that cell death, microglial activation, and synaptic degeneration phenotypes are persistent, which coincides with increased NSPC proliferation. Newborn neurons also survive for long periods (3 months; Figures 2K and 2L). Thus, in contrast to human brains, where Aβ42 deposition impairs stem cell function and neurogenesis,

(M) Quantification for (J–L').
(N) IHC for HuC/D and TR-Aβ42 coupled to TUNEL staining.
(O) Categorization of TUNEL-positive cells according to HuC/D expression and presence of Aβ42.
Scale bars, 100 μm. Data are represented as mean ± SD; n = 3 fish. *p < 0.05; **p < 0.01; ***p < 0.001. See also Figures S1–S3.

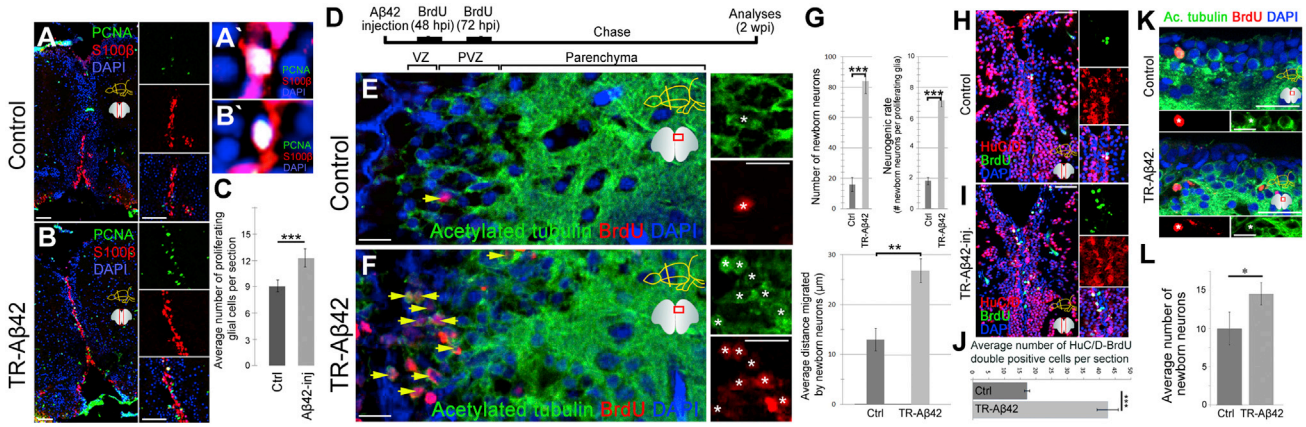

Figure 2. Aβ42 Induces Stem Cell Proliferation and Neurogenesis in Adult Zebrafish Brain

(A) PCNA, S100β and DAPI in control brains. Insets: individual channels.

(A') High-magnification of a double-positive cell.

(B) PCNA, S100β, and DAPI in TR-Aβ42-injected brains.

(B') High-magnification of a double positive cell.

(C) Quantification for the average number of proliferating glial cells. Ctrl, control; inj, injected.

(D) Neurogenesis assay.

(E and F) Acetylated tubulin and BrdU in control (E) and TR-Aβ42-injected (F) brains. Insets: single channels.

(G) Number and migration distance of newborn neurons.

(H and I) HuC/D and BrdU in control (H) and TR-Aβ42-injected brains at 2 weeks post-injection (wpi).

(J) Quantification of HuC/D-BrdU double-positive cells.

(K) Acetylated tubulin and BrdU in control and TR-Aβ42-injected brains at 3 months after injection. Insets: examples of newborn neurons.

(L) Quantification of acetylated tubulin and BrdU double-positive cells per section.

Scale bars, 50 μm (A and B) and 20 μm (E, F, H, I, and K). Data are represented as mean ± SD; n = 3 fish. *p < 0.05; **p < 0.01; ***p < 0.001. See also Figures S1 and S3 and Table S2.

adult zebrafish brain can induce plasticity and neurogenesis, despite the prevailing toxic environment.

Interleukin-4 Induces Stem Cell Plasticity after Aβ42 Aggregation

To determine the changes in gene expression in zebrafish NSPCs after Aβ42 toxicity, we performed transcriptome analysis. Immune-related signaling pathways were highly enriched (Figure S1T; Table S1). Therefore, to determine whether μg/μØ activity is required for enhanced cell proliferation in fish brain, we injected clodronate liposomes, which kill the μg/μØ (Jenkins et al., 2011) (Figure 3). After TR-Aβ42 and control liposome injection, the number of μg/μØ increases, and clodronate treatment reduces the μg/μØ significantly (Figures 3A–3D, 3F, and 3G). Aβ42-induced NSPC proliferation is reduced significantly in clodronate-injected brains (Figures 3E and 3F'). Additionally, quantification of the total PCNA-positive cells showed that overall cell proliferation, which is increased by TR-Aβ42, was reduced to control levels with clodronate. These results indicate that immune activity is required for induced NSPC plasticity upon Aβ42-induced neurodegeneration in adult zebrafish brain. Transcriptome analyses showed that interleukin-4 (IL4) is upregulated in fish brain after Aβ42 injection (Figure S1T). Compared to control brains (Figures 4A–4A''), TR-Aβ42 injection induces IL4 (Figures 4B–4B''), suggesting that IL4 may constitute a specific signaling associated with neurodegeneration in zebrafish brain. We found that neurons and μg/μØ express IL4 (Figures 4C and 4C') and that the majority of the IL4-positive cells are Aβ42-containing neurons (Figure 4C'). The receptor *il4r* is expressed in ventricular cells (Figures 4D–4D''), suggesting a role for IL4 in establishing a crosstalk mechanism between NSPCs and the neurodegenerative milieu.

To test whether IL4 is sufficient to induce proliferation, we injected human IL4 into healthy adult zebrafish brains. Compared to controls (Figures 4E and 4H), IL4 significantly increased NSPC proliferation and neurogenesis (Figures 4F, 4G, 4I, and 4J). To check whether IL4 is necessary for enhanced progenitor cell proliferation, we used an IL4-neutralizing antibody (Acosta-Rodriguez et al., 2007), which detects zebrafish IL4 (Figures 4K and 4K') and, when injected into zebrafish brain, can target the ventricular region containing NSPCs (Figures 4L and 4L'). Compared to TR-Aβ42 injection only, proliferation of NSPCs is reduced after co-injection of TR-Aβ42 and the neutralizing antibody (Figures 4M–4O). To test whether the neutralizing antibody is specifically acting on IL4, we performed a control experiment where co-injection of the neutralizing antibody with IL4 into healthy fish brains resulted in the abrogation of IL4-induced proliferation (Figures S4A–S4D), suggesting a specific knockdown on IL4.

IL4 is known to induce phosphorylation of transcription factor STAT6. Compared to control brains (Figure 4P), TR-Aβ42 and IL4 induced STAT6 phosphorylation (Figures 4P' and 4P''), which can be blocked by antagonizing IL4 (nIL4ab; Figure 4P'''). Thus, STAT6 phosphorylation is downstream to IL4 signaling in NSPCs in adult zebrafish brain.

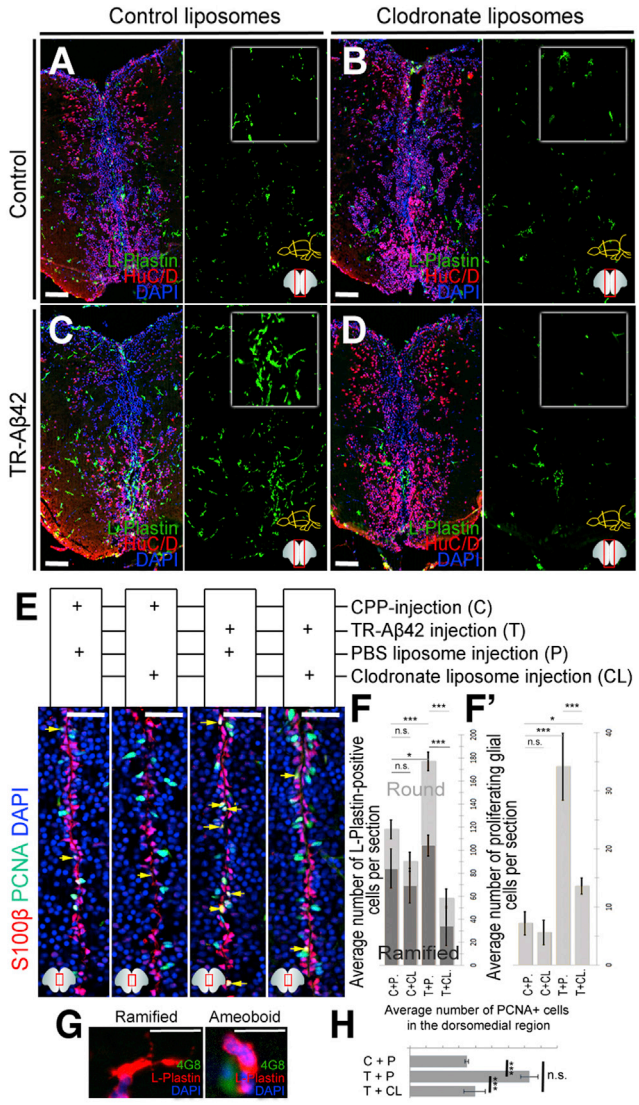

Figure 3. Aβ42-Dependent Stem Cell Proliferation Requires Microglial Activity

(A–D) L-plastin and HuC/D in control peptide/control liposome (A), control peptide/clodronate liposome (B), TR-Aβ42/control liposome (C), and TR-Aβ42/clodronate liposome (D) injections. Right panels: green channel.

(E) S100β and PCNA in brains injected with the four combinations in (A–D).

(F) Quantification of the number of L-plastin-positive cells.

(F') Quantification of proliferating NSPCs.

(G) Examples of ramified and round/ameoboid L-plastin-positive cells. Round cells are around amyloid (green, 4G8 staining).

(H) Quantification for the average number of PCNA-positive cells in clodronate-injected brains.

Scale bars, 50 μm. Data are represented as mean ± SD; n = 4 fish. *p < 0.05; ***p < 0.001; n.s., not significant. See also Tables S1 and S2.

IL4 acts together with IL13 to form dimers that bind to the IL4 receptor (Wang and Secombes, 2015). To test whether IL13 acts similarly to IL4 in mediating radial glial cell proliferation in zebrafish brain, we injected interleukin-13 (IL13) into healthy brains. IL13 only slightly increased NSPC proliferation in adult zebrafish brain (Figures S4E–S4G), suggesting that IL4 is the major component that regulates progenitor cell proliferation in the IL4/IL13 signaling pathway.

The knockdown of IL4 receptor using morpholinos led to the reduction of NSPC proliferation similar to that of the neutralizing antibody (Figures 4Q–4S). Additionally, expression of IL4 after Aβ42 is reduced by clodronate treatment (Figures 4T and 4U), and exogenous IL4 significantly increased the reduced NPSC proliferation after macrophage depletion by clodronate (Figures 4V–4Z). These findings show that Aβ42 toxicity induces progenitor cells through a neuron-glia-immune crosstalk mediated by IL4/STAT6 signaling.

To test whether the IL4 signaling is specific to amyloid toxicity, but not other means of neuronal loss, we checked IL4 expression in brains that are traumatically lesioned. IL4 is not expressed in controls, while in lesioned brains, expression is low and in very few cells that cannot account for a major signaling pathway for induced regeneration (Figures S4H and S4I). Additionally, a specific molecular program activated after traumatic lesions in zebrafish brain—*gata3* expression—is not activated after Aβ42-mediated neurodegeneration (Figure S4J), suggesting that different specific molecular programs could govern the regenerative ability of zebrafish brain after different modes of neuronal loss. Thus, IL4 signaling might be a specific, but not a generic, type of regeneration response after Aβ42-mediated neurodegeneration.

IL4 mediates neuronal survival or microglial dynamics during neurodegeneration (de Araujo et al., 2009). Microglial expression of IL4 seems to positively affect hippocampal cell proliferation (Nunan et al., 2014), while IL4 attenuates Alzheimer-like phenotypes in APP1/PS1 mice by reducing the microgliosis (Kiyota et al., 2010), suggesting that the effects of IL4 on NSPCs and the microglia in constitutive neurogenesis and disease states differ. Furthermore, the beneficial effect of IL4 is likely to be indirect on mammalian NSPC proliferation and is due to the inactivation of microglia, which repress NSPC proliferation in mammalian brains (Das and Basu, 2008; Ekdahl et al., 2009; Monje et al., 2003). Thus, the effects of IL4 were mostly related to altered microglial environment and its effects on NSPCs. However, our studies show that IL4 directly acts on NSPCs.

In zebrafish, inflammation acts as a "positive cue" for neuroregeneration (Kizil et al., 2012a, 2012c, 2015b; Kyritsis et al., 2012, 2014), while in humans, this is not the case, possibly due to cumulative effects of positive and negative cues. Zebrafish, as a valuable reductionist model, thus, could help us to directly address the role of individual factors on stem cells and distinguish the positive and negative inflammatory cues, which could be tested in mammalian systems to find candidates for clinical trials. This understanding may help designing regenerative therapies in neurodegenerative environment of human brains by tweaking the inflammatory milieu and its players, such as IL4.

EXPERIMENTAL PROCEDURES

Ethics Statement

All animal experiments were carried out in accordance with permits of the Landesdirektion Sachsen, Germany (TVV-52/2015) and with the official regulatory standards of the Department of Essonne, France (agreement number A91-577).

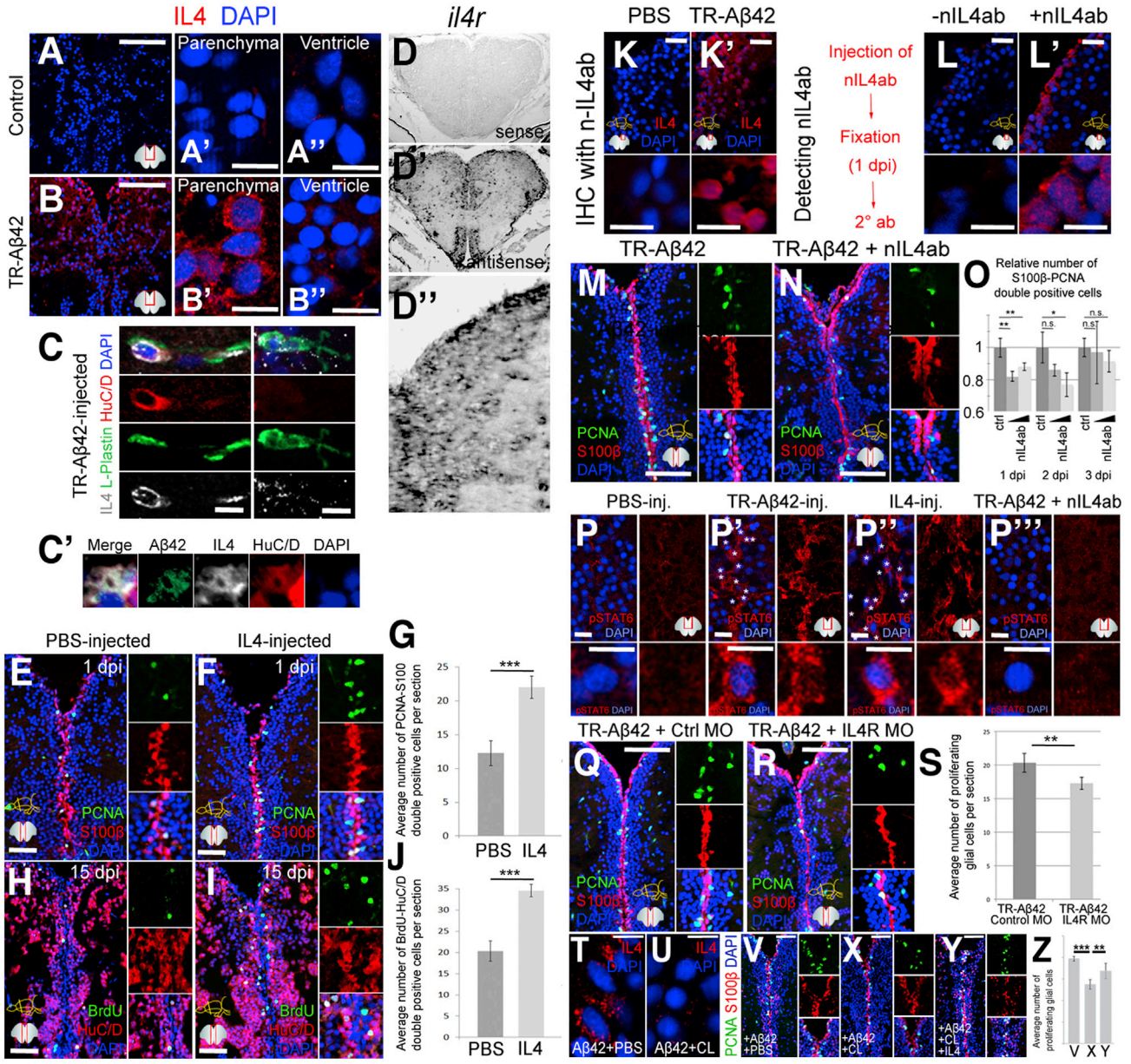

Figure 4. Interleukin-4 Is Necessary and Sufficient for Aβ42-Dependent Stem Cell Proliferation and Neurogenesis in Adult Zebrafish Brain

(A–B'') IL4 in control (A–A'') and TR-Aβ42-injected (B-B'') brains. Parenchyma (A' and B') and ventricle (A'' and B'') are shown.

(C) IL4, L-plastin, and HuC/D in TR-Aβ42-injected brains.

(C') Close-up on a neuron (HuC/D-positive, red) with TR-Aβ42 (green) and IL4 (white).

(D–D'') *il4r* receptor expression in TR-Aβ42 brains at 3 dpi. Sense (D) and antisense (D'). (D'') High magnification.

(E and F) S100β and PCNA in control (E) and IL4-injected (F) brains.

(G) Quantification graph for (E and F).

(H and I) BrdU and HuC/D in control (H) and IL4-injected (I) brains.

(J) Quantification graph for (H and I).

(K and K') IL4 detection with neutralizing antibody in control (K) and TR-Aβ42-injected (K') brains.

(L and L') Secondary antibody staining for the neutralizing IL4 antibody (nIL4ab) in uninjected (L) and injected brains at 1 day after injection (L').

(M and N) PCNA and S100β in TR-Aβ42-injected (M) and in TR-Aβ42 + neutralizing antibody-co-injected (N) brains. Insets: single fluorescence channels.

(O) Quantification graph. Control = 1.

(P–P''') Phospho-STAT6 in PBS- (P), TR-Aβ42- (P'), IL4- (P''), and TR-Aβ42 + neutralizing IL4-antibody-injected (P''') brains. Red channels shown separately. Insets: close-up image of one exemplary cell.

(Q–S) PCNA and S100 in TR-Aβ42 and control morpholino-injected (Q) and in TR-Aβ42 and IL4R morpholino-injected (R) brains. (S) Quantification graph.

(legend continued on next page)

Peptide Synthesis

Peptides (Table S2) were synthesized using 9-fluorenylmethoxycarbonyl (Fmoc) chemistry with 2-(1H-benzotriazol-1-yl)-1,1,3,3-tetramethyluronoium-hexafluorphosphate (HBTU) activation on an automated solid-phase peptide synthesizer (ResPep SL, Intavis). The peptide was cleaved from the resin with trifluoroacetic acid (TFA)/tri-isopropylsilane (TIS)/water/DTT (90 [v/v]: 5 [v/v]: 2.5 [v/v]: 2.5 [m/v]) and was precipitated with ice-cold diethyl ether.

The peptides were dissolved in 1:1 Milli-Q water:acetonitrile and purified via reverse-phase high pressure liquid chromatography (HPLC) on a semi-preparative HPLC column (Waters) equipped with a porous polystyrene divinylbenzene column (PolymerX; bead size, 10 μm, 250 mm × 10 mm; Phenomenex). Purity was confirmed by analytical reverse-phase ultra-HPLC (UPLC Aquity with UV Detector), using an analytical C18 column (bead size, 1.7 μm), and the peptide products were characterized by electrospray ionization-mass spectrometry (ESI-MS; ACQUITY TQ Detector) (Figure S1).

CD Spectroscopy

CD spectra were recorded using Chirascan Plus (Applied Photophysics). The experiments were performed at a 20 μM concentration in water or 10 mM sodium phosphate buffer (pH 8.0) incubated at 37°C. The spectra were recorded using a quartz cuvette of 0.1 cm path length in the far-UV range (190–260 nm), applying a scanning rate of 120 nm/min. For a typical spectrum, five scans were averaged, and the baseline was corrected.

Light Scattering

The experiments were performed at 20 μM concentration in water or 10 mM sodium phosphate buffer (pH 8.0). Turbidity was measured at room temperature with orbital shaking in half-area, nonbinding-surface, 384-well plates (Greiner) on a plate reader (Paradigm, Beckman Coulter). The total volume was 60 μL, and the experiments were performed in triplicate.

Microinjections

Cerebroventricular microinjections (CVMIs) were performed as described elsewhere (Kizil and Brand, 2011; Kizil et al., 2015a). 2 μL peptides (20 μM), PBS, clodronate liposomes (1 mg/mL), and neutralizing antibody for IL4 (Novus Biological; MAB204; 10 μg/mL), human IL4, and IL13 (R&D Systems, 1 μg/mL) were injected. An antisense morpholino (5′-AGGCAAGTA CAAACACTCACTCATA-3′; Gene Tools) directed against zebrafish *il4r* (ENSDARG00000102583) was injected at a 10 μM concentration.

Tissue Preparation and Immunohistochemistry

Tissue preparations and stainings were performed as previously described (Kizil et al., 2012c, 2014), using various antibodies (Table S1).

Transmission Electron Microscopy

Fish brains were immersed in modified Karnovsky's fixative (2% glutaraldehyde, 2% paraformaldehyde in 50 mM HEPES) overnight at 4°C. Samples were postfixed in 1% OsO_4/water for 2 hr on ice, en bloc contrasted with 1% uranyl acetate/water for 2 hr on ice, and dehydrated in a graded series of ethanol. Brains were infiltrated in epon gradient, embedded in flat embedding molds, and cured at 65°C. Ultrathin sections were prepared with Leica UC6 ultramicrotome (Leica Microsystems), collected on formvar-coated slot grids, stained with lead citrate and uranyl acetate as described elsewhere (Venable and Coggeshall, 1965), and analyzed on a Morgagni 268D transmission electron microscope (FEI) at 80 kV acceleration voltage.

BrdU Experiments

Zebrafish were immersed in freshly prepared 10 mM BrdU (Sigma-Aldrich) solution in E3 for 8 hr/day at 48 and 72 hours post-infection (hpi). Fish were sacrificed, and heads were subjected to histological preparations as described previously (Kizil et al., 2012c).

Imaging and Statistical Analyses

Images were acquired using a Zeiss AxioImager Z1. Only sections between the caudal end of the olfactory bulb and anterior commissure were counted. The quantification of the average signal intensities and synaptophysin-positive synapses were performed using a 3D object counter module of ImageJ software. Cell counting was performed manually. The statistical evaluation was performed using GraphPad Prism (version 6.02) for one-way ANOVA, followed by a Tukey's post hoc test, and for Student's t test. Error bars shown indicate the SEM, and asterisks indicate significance: *$p < 0.05$, **$p < 0.01$, and ***$p < 0.001$. $p > 0.05$ is considered not significant (n.s.). Student's t test was performed for paired samples, and a t test was performed for independent measurements.

ACCESSION NUMBERS

The accession number for next-generation sequencing results reported in this paper is GEO: GSE74326.

SUPPLEMENTAL INFORMATION

Supplemental Information includes Supplemental Experimental Procedures, four figures, and two tables and can be found with this article online at http://dx.doi.org/10.1016/j.celrep.2016.09.075.

AUTHOR CONTRIBUTIONS

P.B. and C.K. performed injections, tissue preparation, sectioning, and antibody staining. A.K.T. and Y.Z. synthesized the peptides and performed CD analyses. M.I.C., C.P., and V.M. performed sectioning and tissue isolation. C.F. performed the passive avoidance test. S.R. and A.D. performed transcriptome sequencing. T.K. prepared samples and performed transmission electron microscopy. C.K. and P.B. conceived and designed the experiments, analyzed the data, and wrote and edited the manuscript.

ACKNOWLEDGMENTS

This work was supported by DZNE, the Helmholtz Association (VH-NG-1021), CRTD, TU Dresden (FZ-111, 043_261518), and DFG (KI1524/6) (C.K.); and by the Leibniz Association (SAW-2011-IPF-2) and BMBF (BioLithoMorphie 03Z2E511) (A.K.T. and Y.Z.). We would like to thank Dr. Laure Bally-Cuif for suggestions and comments, Dr. Alessandro Alunni for help with fish work, and Ulrike Hoffman for peptide synthesis.

Received: October 21, 2015
Revised: June 25, 2016
Accepted: September 22, 2016
Published: October 18, 2016

REFERENCES

Acosta-Rodriguez, E.V., Napolitani, G., Lanzavecchia, A., and Sallusto, F. (2007). Interleukins 1beta and 6 but not transforming growth factor-beta are essential for the differentiation of interleukin 17-producing human T helper cells. Nat. Immunol. *8*, 942–949.

Ben-Hur, T., Ben-Menachem, O., Furer, V., Einstein, O., Mizrachi-Kol, R., and Grigoriadis, N. (2003). Effects of proinflammatory cytokines on the growth, fate, and motility of multipotential neural precursor cells. Mol. Cell. Neurosci. *24*, 623–631.

Chapouton, P., Jagasia, R., and Bally-Cuif, L. (2007). Adult neurogenesis in non-mammalian vertebrates. BioEssays *29*, 745–757.

(T and U) IL4 after TR-Aβ42 in PBS (T) or clodronate-injected (U) brains.
(V–Z) PCNA and S100 after TR-Aβ42 in PBS (V), clodronate (X) or clodronate + IL4-injected (Y) brains. (Z) Quantification graph for (V–Y).
Scale bars, 50 μm (A, B, E–I, M, N, Q, R,V–Y), 10 μm (A', A'', B', B''', C, P–P''', T, and U), and 20 μm (K–L'). Data are represented as mean ± SD; n = 4 fish. *$p < 0.05$; **$p < 0.01$; ***$p < 0.001$; n.s., not significant. See also Figure S4.

Chen, G., Chen, K.S., Knox, J., Inglis, J., Bernard, A., Martin, S.J., Justice, A., McConlogue, L., Games, D., Freedman, S.B., and Morris, R.G. (2000). A learning deficit related to age and beta-amyloid plaques in a mouse model of Alzheimer's disease. Nature *408*, 975–979.

Cosacak, M.I., Papadimitriou, C., and Kizil, C. (2015). Regeneration, plasticity, and induced molecular programs in adult zebrafish brain. BioMed Res. Int. *2015*, 769763.

Das, S., and Basu, A. (2008). Inflammation: a new candidate in modulating adult neurogenesis. J. Neurosci. Res. *86*, 1199–1208.

de Araujo, E.G., da Silva, G.M., and Dos Santos, A.A. (2009). Neuronal cell survival: the role of interleukins. Ann. N Y Acad. Sci. *1153*, 57–64.

Demars, M., Hu, Y.S., Gadadhar, A., and Lazarov, O. (2010). Impaired neurogenesis is an early event in the etiology of familial Alzheimer's disease in transgenic mice. J. Neurosci. Res. *88*, 2103–2117.

Doetsch, F., García-Verdugo, J.M., and Alvarez-Buylla, A. (1997). Cellular composition and three-dimensional organization of the subventricular germinal zone in the adult mammalian brain. J. Neurosci. *17*, 5046–5061.

Duff, K., Eckman, C., Zehr, C., Yu, X., Prada, C.M., Perez-tur, J., Hutton, M., Buee, L., Harigaya, Y., Yager, D., et al. (1996). Increased amyloid-beta42(43) in brains of mice expressing mutant presenilin 1. Nature *383*, 710–713.

Ekdahl, C.T., Kokaia, Z., and Lindvall, O. (2009). Brain inflammation and adult neurogenesis: the dual role of microglia. Neuroscience *158*, 1021–1029.

Haass, C., and Selkoe, D.J. (2007). Soluble protein oligomers in neurodegeneration: lessons from the Alzheimer's amyloid beta-peptide. Nat. Rev. Mol. Cell Biol. *8*, 101–112.

Jenkins, S.J., Ruckerl, D., Cook, P.C., Jones, L.H., Finkelman, F.D., van Rooijen, N., MacDonald, A.S., and Allen, J.E. (2011). Local macrophage proliferation, rather than recruitment from the blood, is a signature of TH2 inflammation. Science *332*, 1284–1288.

Kiyota, T., Okuyama, S., Swan, R.J., Jacobsen, M.T., Gendelman, H.E., and Ikezu, T. (2010). CNS expression of anti-inflammatory cytokine interleukin-4 attenuates Alzheimer's disease-like pathogenesis in APP+PS1 bigenic mice. FASEB J. *24*, 3093–3102.

Kizil, C., and Brand, M. (2011). Cerebroventricular microinjection (CVMI) into adult zebrafish brain is an efficient misexpression method for forebrain ventricular cells. PLoS ONE *6*, e27395.

Kizil, C., Dudczig, S., Kyritsis, N., Machate, A., Blaesche, J., Kroehne, V., and Brand, M. (2012a). The chemokine receptor cxcr5 regulates the regenerative neurogenesis response in the adult zebrafish brain. Neural Dev. *7*, 27.

Kizil, C., Kaslin, J., Kroehne, V., and Brand, M. (2012b). Adult neurogenesis and brain regeneration in zebrafish. Dev. Neurobiol. *72*, 429–461.

Kizil, C., Kyritsis, N., Dudczig, S., Kroehne, V., Freudenreich, D., Kaslin, J., and Brand, M. (2012c). Regenerative neurogenesis from neural progenitor cells requires injury-induced expression of Gata3. Dev. Cell *23*, 1230–1237.

Kizil, C., Kuchler, B., Yan, J., Ozhan, G., Moro, E., Weidinger, G., Brand, M., and Antos, C.L. (2014). Simplet/Fam53b is required for beta catenin nuclear translocation in zebrafish development. Development *141*, 3529–3539.

Kizil, C., Iltzsche, A., Thomas, A.K., Bhattarai, P., Zhang, Y., and Brand, M. (2015a). Efficient cargo delivery into adult brain tissue using short cell-penetrating peptides. PLoS ONE *10*, e0124073.

Kizil, C., Kyritsis, N., and Brand, M. (2015b). Effects of inflammation on stem cells: together they strive? EMBO Rep. *16*, 416–426.

Kokaia, Z., Martino, G., Schwartz, M., and Lindvall, O. (2012). Cross-talk between neural stem cells and immune cells: the key to better brain repair? Nat. Neurosci. *15*, 1078–1087.

Kyritsis, N., Kizil, C., Zocher, S., Kroehne, V., Kaslin, J., Freudenreich, D., Iltzsche, A., and Brand, M. (2012). Acute inflammation initiates the regenerative response in the adult zebrafish brain. Science *338*, 1353–1356.

Kyritsis, N., Kizil, C., and Brand, M. (2014). Neuroinflammation and central nervous system regeneration in vertebrates. Trends Cell Biol. *24*, 128–135.

Monje, M.L., Toda, H., and Palmer, T.D. (2003). Inflammatory blockade restores adult hippocampal neurogenesis. Science *302*, 1760–1765.

Nunan, R., Sivasathiaseelan, H., Khan, D., Zaben, M., and Gray, W. (2014). Microglial VPAC1R mediates a novel mechanism of neuroimmune-modulation of hippocampal precursor cells via IL-4 release. Glia *62*, 1313–1327.

Schwartz, M., and Shechter, R. (2010). Systemic inflammatory cells fight off neurodegenerative disease. Nat. Rev. Neurol. *6*, 405–410.

Selkoe, D.J. (2002). Alzheimer's disease is a synaptic failure. Science *298*, 789–791.

Shaked, G.M., Kummer, M.P., Lu, D.C., Galvan, V., Bredesen, D.E., and Koo, E.H. (2006). Abeta induces cell death by direct interaction with its cognate extracellular domain on APP (APP 597-624). FASEB J. *20*, 1254–1256.

Tanaka, E.M., and Ferretti, P. (2009). Considering the evolution of regeneration in the central nervous system. Nat. Rev. Neurosci. *10*, 713–723.

Venable, J.H., and Coggeshall, R. (1965). A simplified lead citrate stain for use in electron microscopy. J. Cell Biol. *25*, 407–408.

Wang, T., and Secombes, C.J. (2015). The evolution of IL-4 and IL-13 and their receptor subunits. Cytokine *75*, 8–13.

Wyss-Coray, T. (2006). Inflammation in Alzheimer disease: driving force, bystander or beneficial response? Nat. Med. *12*, 1005–1015.